Measurements of Thermal Diffusivity of Molten InGaAs by the Laser Flash Method

Toshio Nagashima† and Hirokazu Katoh†
Yoshio Hayashi†† and Harunobu Hayakawa††
Kyoichi Kinoshita(†††, ††††)

† Space Utilization Research Center, National Space Development Agency of Japan, 2-1-1, Sengen, Tsukuba, Ibaraki, 305-8505, Japan

†† Space Station Group, Advanced Engineering Services Co.,Ltd. 1-6-1, Takezono, Tsukuba, Ibaraki, 305-0032, Japan

††† Space Utilization Research Program, National Space Development Agency of Japan, 2-1-1, Sengen, Tsukuba, Ibaraki, 305-8505, Japan

†††† NTT Basic Research Laboratories, 3-1, Morinosato, Wakamiya, Atsugi, 243-0198, Japan

Thermal diffusivity of molten $In_{0.8}Ga_{0.2}As$ was measured using the laser-flash method. The sample $In_{0.8}Ga_{0.2}As$ was sandwiched between thin graphite disks, and sealed in a transparent quartz container with a flat window of sufficient strength to withstand the high-vapor pressure of arsenic. As a result, a three-layerd cell was formed.
Thermal diffusivity of molten $In_{0.8}Ga_{0.2}As$ was 10～12 mm^2/s from melting point to 1150℃. Scattering of the measured thermal diffusivity was less than 5%.

1. Introduction

Thermal diffusivity is an important thermophysical property to be taken into consideration in space experiments where heat transport by thermal convection is suppressed.

InGaAs is paid special attention in recent years as high speed ICs and optoelectronic materials such as laser diodes [1]. However, growth of the ternary compound semiconductor with high uniform monocrystallinity is difficult on the ground. Although utilizing microgravity environments upon crystal growth is expected for the detailed characteristic research, only a few reports have been published on the thermophysical properties of molten InGaAs [2) 3)]. No report has been published on the thermal diffusivity of molten InGaAs.

In this paper , we report thermal diffusivity of molten $In_{0.8}Ga_{0.2}As$.

2. Experimental method

Thermal diffusivity was measured by the laser flash method. The schematic diagram of the experimental apparatus is shown in Fig. 1.

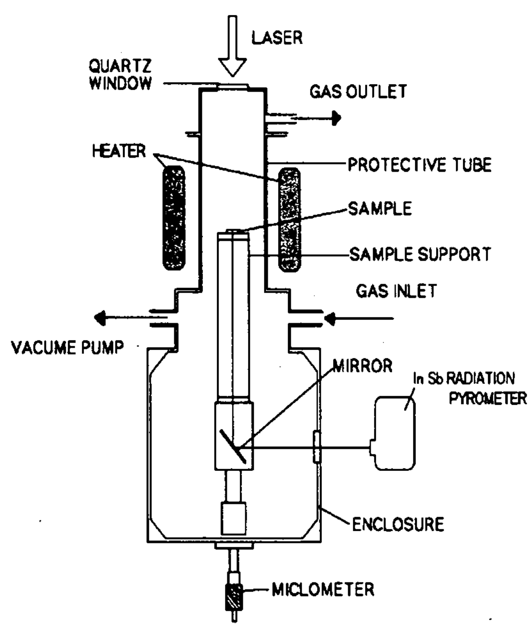

Fig.1 Schematic Diagram of the experimental apparatus

Figure 2 shows the quartz container with the specimen. The sample (ϕ 10×1～3mm^t) was sandwiched between thin graphite disks (ϕ 10× 0.2mm^t), and sealed in a transparent quartz container with a flat window of sufficient strength to withstand the high-vapor pressure of arsenic. Figure 3 shows a model of the specimen. The front surface of layer 2 is heated by a laser-pulse. The radiative signals from both the rear surface of layer 3 and layer 4 are measured by an IR detector.

When the thickness of the quartz at the rear surface of the specimen is thick enough for thermal diffusivity ratio α_2/α_4, the effect of quartz container is removed [4]. As a result, a three-layerd cell was formed.

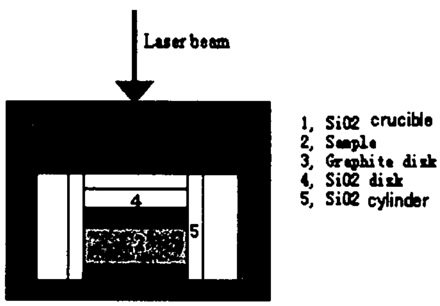

Fog.2 Quartz container

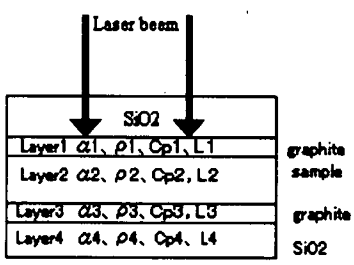

Fig.3 Model of a specimen

The theoretical curve of time-temperature history of the rear surface of the layer 3 is introduced by equation(1) and thermal diffusivity is calculated [5) 6)].

$$\nu = 1 + 2^{\infty}\Sigma_{k=1}\left[\left(\omega_1 X_1 + \omega_2 X_2 + \omega_3 X_3 + \omega_4 X_4\right)\right] \cdot \exp\left(-\gamma_k^2 t / \eta_3^2\right) / \left\{ \begin{array}{l} \omega_1 X_1 \cos(\omega_1\gamma_k) + \omega_2 X_2 \cos(\omega_2\gamma_k) \\ + \omega_3 X_3 \cos(\omega_3\gamma_k) + \omega_4 X_4 \cos(\omega_4\gamma_k) \end{array} \right\} \quad \cdots(1)$$

$x_1=H_{1/3}\eta_{3/1}+H_{1/2}\eta_{2/1}+H_{2/3}\eta_{3/2}+1 \quad \omega_1=\eta_{1/3}+\eta_{2/3}+1$
$x_2=H_{1/3}\eta_{3/1}-H_{1/2}\eta_{2/1}+H_{2/3}\eta_{3/2}-1 \quad \omega_2=\eta_{1/3}+\eta_{2/3}-1$
$x_3=H_{1/3}\eta_{3/1}-H_{1/2}\eta_{2/1}-H_{2/3}\eta_{3/2}+1 \quad \omega_3=\eta_{1/3}-\eta_{2/3}+1$
$x_4=H_{1/3}\eta_{3/1}+H_{1/2}\eta_{2/1}-H_{2/3}\eta_{3/2}-1 \quad \omega_4=\eta_{1/3}-\eta_{2/3}-1$
$H_j=\rho_\varphi\chi_{\pi\varphi}\Lambda_\varphi \quad \eta_\varphi=L_j/\alpha_\varphi^{1/2} \quad H_{i/j}=H_i/H_j \quad \eta_{i/j}=\eta_i/\eta_j$
(i,j=1,2,3)
ρ : density, C_p : heat capacity, L : thickness,
α : thermal diffusivity,
γ_k : k-th positive root of the characteristic equation.
$x_1\sin(\omega_1\gamma)+x_2\sin(\omega_2\gamma)+x_3\sin(\omega_3\gamma)+x_4\sin(\omega_4\gamma)=0$

$Cp_{graphite}$ [7)] $=-8\times10^{-7}(T(K)-273)^2+0.002T+0.7358$
(J/g·K) ···(2)

Cp_{Ga} [8)] $=0.399$
(J/g·K) ···(3)

$Cp_{In0.8Ga0.2As}$ [9)] $=0.364$
(J/g·K) ···(4)

(calculation value by molar ratio of GaAs/InAs)

$\rho_{graphite}=1.79$ (at R. T.)
(g/cm^3) ···(5)

ρ_{Ga} [10)] $=6.09-0.0006(T(K)-29.8)$
(g/cm^3) ···(6)

$\rho_{In0.8Ga0.2As}$
$=5.6691+0.00052496T(℃)-4.7518\times10^{-7}T(℃)^2$
(g/cm^3) ···(7)

(γ-ray attenuation method)

$\alpha_{graphite}$
$=2\times10^{-12}(T(K)-273)^4-6\times10^{-9}(T(K)-273)^3$
$+7\times10^{-6}(T(K)-273)^2-0.0039(T(K)-273)+1.031$
(cm^2/s) ···(8)

3. Results

The thermal diffusivity of molten Ga

Figure 4 shows measured thermal diffusivity of Ga. In this experiment the range of specimen thickness was between 1 and 2mm and the thickness of the quartz at the rear surface of the specimen is 2mm.

Thermal diffusivity of molten Ga presented in this work is in good agreement with the reported values [4) 11)].

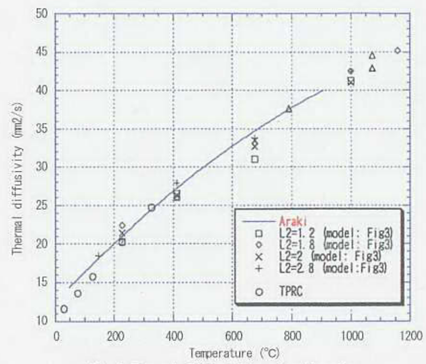

Fig. 4 Thermal diffusivity of molten Ga

Fig.4 Thermal diffusivity of molten Ga

The thermal diffusivity of molten InGaAs

Figure 5 shows measured thermal diffusivity of InGaAs. The data shown here were obtained with specimens of 1mm thickness and the thickness of the quartz at the rear surface of the specimen is 4mm.

Thermal diffusivity of molten InGaAs presented in this work is larger than the value estimated by A. S. Jordan [12)] but in good agreement with those estimated by the Wiedemann-Franz Law [9) 13) 14)]. Scattering of the measured values at the same temperature was less than 5% in this experiment.

4. Summary

Thermal diffusivity of molten In0.8Ga0.2As was measured for the first time in the temperature range between 1040 and 1150 ℃. It gradually increased from 10 to 12 mm2/s with increasing temperature. The data are useful for optimizing crystal growth conditions as well as improving the numerical analysis.

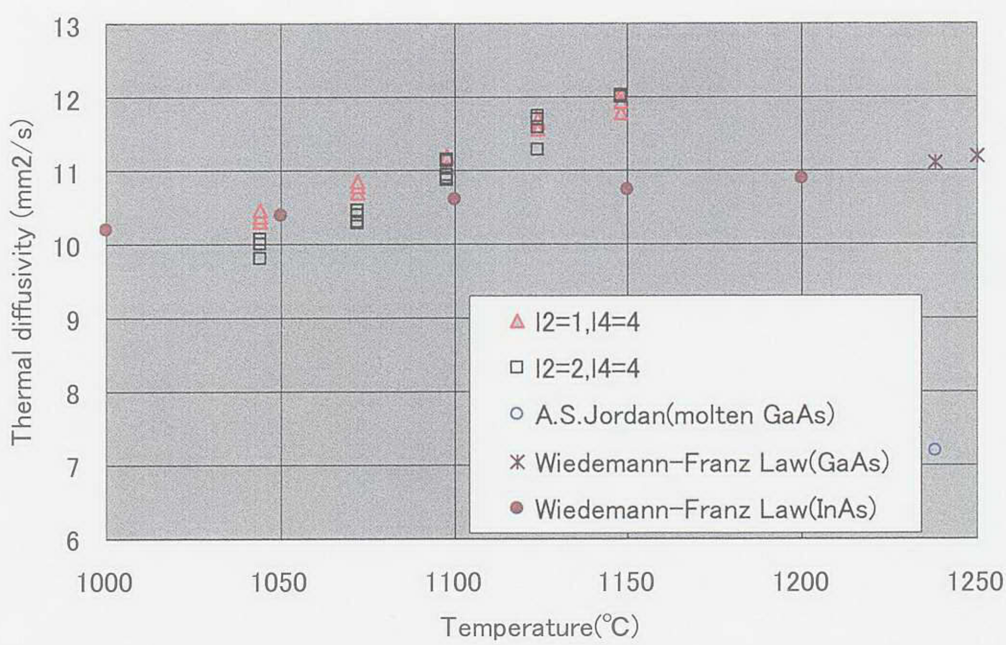

Fig. 5 Thermal diffusivity of molten In0.8Ga0.2As

Reference

1) S. Fujiwara, T. Araki, M. Tatsumi, M. Irikura, K. Matsumoto, S. Murai, J. Crystal Growth, 167 (1996) 357
2) Y. Hayasaka, K. Edamura, M. Iwai, N. Onogawa, K. Kinoshita, J. Jpn. Soc. Microgravity Appl, 14-4(1997) 304
3) T. Nagashima, H. Katoh, Y. Saita, T. Satoh, K. Kinoshita, J. Jpn. Soc. Microgravity Appl, 16-4(1999) 295
4) N.Araki, Y.Tozawa, DaWei Tang, Y.Hayakawa, Proc. 20th Jpn Symp. Thermophys. Prop., Tokyo, 1999, 284-287
5) N.Araki, R. E. Taylor, 15th Jpn Symp Thermophys. Prop, 1978, 469
6) N.Araki, R. E. Taylor, 2th Jpn Symp. Thermophys. Prop, 1981, 9
7) Ishikawa, Nagaoki, New Carbon Industry(1986)
8) International Tables of selected Constants 16, Metals, Thermal and Mechanical Data.
9) K. Yamaguchi, K. Itagaki, A. Yazawa, J.Japan Inst. Metals, 53, 8(1989), 764-770
10) Metals Reference Book, 5^{th} ed.(1976), Butterworths.
11) The TPRC Date Series, Thermophysical Properties of Matter, Vol10, 68,79, Plenum (1973)
12) A. S. Jordan, J. of Crystal Growth, 71 (1985), 551-558
13) O.Madelung, M. Schulz, H. Weiss, Landolt-Börnstein, Numerical Data Functional Relationships Science Technology, 338
14) V. M. Glazov et al, Liquid Semiconductors, Plenum, NY, (1969), 124